An Experimental Investigation on the Mechanism of Tollmien-Schlichting Waves for a NACA 0012 Aerofoil

B. Zang*, Yannick D. Mayer† and Mahdi Azarpeyvand‡

Faculty of Engineering, University of Bristol, United Kingdom

The present study investigates experimentally on the development of Tollmiem-Schlicting (T-S) instabilities and its associated aerofoil noise using a highly instrumented NACA 0012 profile with four angles of attack (α = 0°, 2°, 4° and 6°) at moderate Reynolds numbers, ranging from 1.8×10^5 to 4.6×10^5 based on the chord length. The measured far-field noise spectra captured clearly both the broadband and multiple discrete tonal noises centred around a dominant peak, consistent with the existing literatures. Examinations on the near-field pressure and wake velocity spectra suggests that the dominant tones and its harmonics propagate over the entire flow field, extending both upstream to the leading-edge as well as downstream beyond the near-wake region, which agrees with the characteristics of vortex noise as proposed by Paterson et al.[1] On the other hand, the dominant tones scale very well with $f = 9.4\,\mathrm{n}U^{0.8}$ across the entire range of flow velocities at lower angles of attack, corroborating with the feedback loop mechanisms derived by Tam.[2] Evidences from the near- and far-field noise measurements prompt further investigations into the correlations between near-field pressure fluctuations and wake velocity. The results suggest not only the existence of periodic large-scale structures, consistent with the characteristics of hydrodynamic instability, but also a phase reversal in the near-wake region close to the aerofoil trailing-edge. The present results demonstrate that the aerofoil noise stemming from T-S instabilities could be attributed to a combination of the vortex disturbances and near-wake feedback loop and their dynamic and complex interactions.

Nomenclature

α	angle of attack [degree (°)]
C	aerofoil chord length $[m]$
f	frequency related to aerofoil noise $[Hz]$
f_n	discrete tonal frequency, related to n $[Hz]$
$f_{n,max}$	dominant tonal frequency $[Hz]$
$f_{n1,max}$	primary tonal frequency $[Hz]$ when harmonics are present
$f_{n2,max}$	secondary tonal frequency $[Hz]$ when harmonics are present
f_s	broadband central frequency $[Hz]$
L	characteristics length in the acoustic feedback loop $[m]$
n	integer number on the feedback model
p_0	reference pressure for PSD calculations $[Pa]$
ϕ_{pp}	PSD of the pressure fluctuations $[dB/Hz]$
ϕ_{uu}	PSD of the wake velocity $[dB/Hz]$
U	free stream velocity $[m/s]$
u	instantaneous velocity $[m/s]$
Re	Reynolds number
Re_c	Reynolds number based on chord length

*Research Associate, Department of Aerospace Engineering, University of Bristol.
†Ph.D. Researcher, Department of Aerospace Engineering, University of Bristol.
‡Reader in Aeroacoustics, Department of Mechanical Engineering, University of Bristol.

$R_{p'u'}$	Temporal correlation of surface pressure and wake velocity
x/C	streamwise distance to chord ratio
PSD	Power Spectral Density $[dB/Hz]$

I. Introduction

The recent spike of interest in the design and development of small-to-medium sized unmanned aerial vehicles has revived extensive research interest into aerofoil noise at moderate Reynolds number. Although aerofoil self-noise is often broadband in nature, discrete tonal noises have been observed as a marked signature when it operates at low-to-moderate Reynolds number. Earlier experimental work performed, such as by Clark[3] and Hersh and Hayden,[4] showed clearly that the measured noise spectrum exhibited distinct frequency peaks, which appeared to dominate the total noise power emitted under certain experimental conditions. Later, Paterson et al.[1] conducted carefully a set of noise measurement on two-dimensional NACA 0012 and NACA 0018 aerofoils and discovered the existence of a 'ladder-type' behaviour of the individual tonal peaks with respect to Reynolds number, up to approximately $Re = 10^6$. Based on the measurements, they proposed two scaling laws of firstly $f \sim U^{1.5}$ on the averaged (i.e. smoothing out all 'sudden' jumps) frequency peaks and more importantly, of $f \sim U^{0.8}$ on the frequency peaks of a particular 'rung' of the ladder structure. Using the results from Paterson et al., Tam[2] suggested a feedback mechanism with the presence of a self-excited feedback loop between the noise source in the wake and the trailing-edge, and also a phase condition necessary for the evolution of discrete frequencies. As such, the discrete tonal frequency follows a law of $f = 6.85nU^{0.8}$. Moreover, Fink[5] demonstrated that the laminar boundary-layer instability analysis predicted very well on the evolution of the averaged tonal peaks over the range of Reynolds numbers. Since such loud discrete tones present notable concerns to the health during the engineering design of helicopter rotors, micro air vehicles and small to medium sized wind turbines,[2,6] significant research efforts have then been devoted towards understanding the mechanism and evolution of these tonal noises,[7–9] and furthermore reducing their strengths with minimal loss on the aerodynamic performance.[10,11]

Arbey and Batalie[12] investigated experimentally the aerofoil noises of both a standard and a modified NACA 0012 profiles immersed in a uniform laminar flow. With improved data-processing resolution, they were able to illustrate that the far-field noise spectrum consists of a superposition of the broadband 'hump' with primary frequency f_s and a series of regularly spaced discrete peaks f_n centred around $f_{n,max}$ peak with the maximum magnitude (see Figure 4 for the identification of the various frequency peaks). Remarkably, through combining the approaches from both Tam[2] and Fink,[5] they identified the broadband component as the diffraction of the Tollmien-Schlicting (T-S) instabilities by the trailing-edge, while the discrete tones arose due to the aeroacoustic feedback mechanism with a characteristic length L, determined from the point of maximum velocity on the surface to the trailing-edge of the aerofoil. The occurrence of T-S instabilities was further confirmed by Lowson et al.[13] when they detected the T-S waves in the boundary layers of the aerofoil before tonal noises could be heard. In addition, Lowson et al. found that the discrete tones were strongly correlated with the appearance of a long laminar separation bubble along the pressure surface of NACA 0012 profile over a range of Reynolds number.

Despite the success of Arbey and Batalies feedback loop model in elucidating the emission mechanism of discrete tonal noises, there are still discrepancies between the predicted and measured frequencies. Moreover, several recent studies have shown mounting evidence on the possible existence of dual feedback loops on both surfaces of an aerofoil in the laminar flow. For instance, Desquesnes et al.[14] performed Direct Numerical Simulations (DNS) of the NACA 0012 aerofoil at two non-zero incident angle of attacks (α). Through the rich flow-field information available from their numerical tests, they concluded that while the feedback mechanism along the pressure surface could account for the primary tone f_s, a secondary feedback loop was observed to produce fluctuations of the hydrodynamic instabilities between the pressure and suction sides, which subsequently generated a periodic amplitude modulation of the primary tone. More interestingly, from detailed Particle Image Velocimetry and acoustic measurements, Probsting et al.[15] revealed that generation of the tonal noise was dominated by the suction surface activity at lower Reynolds number ($Re \sim 30{,}000$) and conversely by the pressure surface activity when the Reynolds number increases, which indicated an elevated level of interactions between the two surfaces. As such, some questions on the dual feedback mechanisms and their likely contributions towards the discrete primary and secondary tones remain open, and furthermore, as pointed out by the Desquesnes et al., experimental studies into the assessment and correlation of the

acoustic characteristics between the trailing-edge and corresponding noise source are still relatively limited.

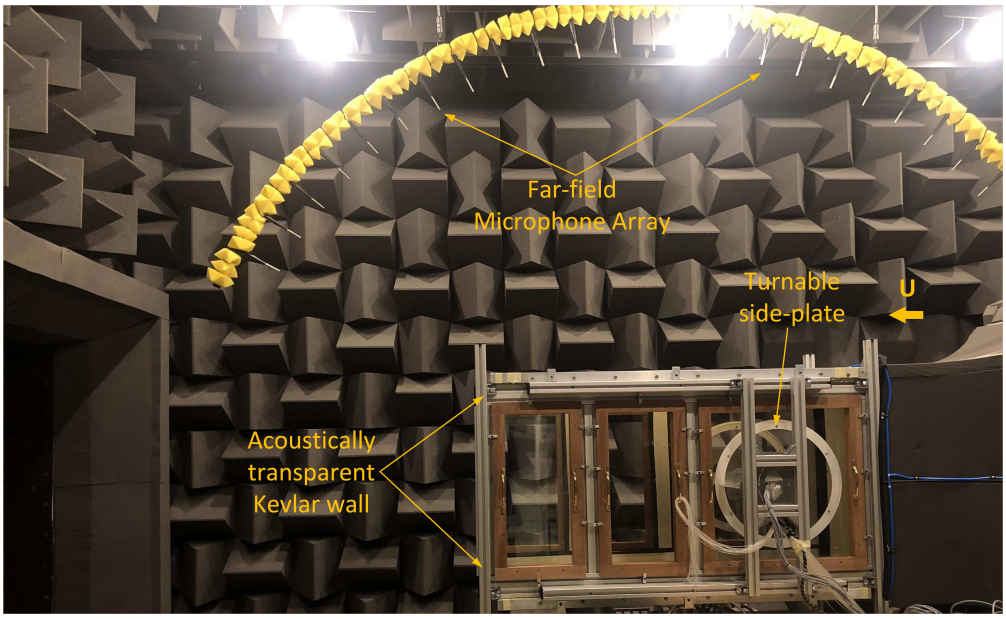

Figure 1: Side view of the test section with NACA 0012 aerofoil inside the anechoic chamber including nozzle, collector and far-field microphone arc.

Therefore, the present work aims to carry out extensive experimental measurements on the near-field (i.e. surface pressure) and far-field tonal noises of a NACA 0012 aerofoil at various angles of attack as well as at moderate Reynolds numbers. The purpose of the study is two-folds: firstly, to shed more light onto the possible feedback mechanisms of the tonal noises through examining the acoustic spectra at multiple locations along both the pressure and suction surfaces, on top of which, correlations between the wake flow and the near- and far-field noise spectra will be studied. Secondly, the present experimental work can serve as a suitable set of validation data for numerical simulations.

II. Experimental setup

The experiments have been performed in the aeroacoustic wind tunnel facility at the University of Bristol.[16] An overview of the test setup inside the anechoic chamber of the wind tunnel can be seen in Figure 1. The NACA 0012 aerofoil was mounted inside a carefully designed Kevlar-walled test section, which has a total length of 1500 mm. Subsequently, the test section is attached air-tight to a nozzle with internal dimensions measuring of 775 mm (H) $\times$ 500 mm (W). At both the top and bottom of the test section, draw-bar T175HD tensioning frames are mounted, allowing the 0.12 mm thick Kevlar®49 cloth to be uniformly tensioned to approximately 20 N cm^{-1}. In order to adjust easily and accurately of the Angles of Attack (hereforth will be referred to as AoAs), the aerofoil was mounted onto the side of the test section via a circular turning plate with a diameter of 460 mm. Last but not least, all internal gaps have been covered to avoid undesirable noise contaminations.

With a chord length (C) of 300 mm, the NACA 0012 aerofoil under the present experiments is equipped with 87 pressure taps of which up to 64 can be connected simultaneously to two MicroDaq-32 pressure acquisition systems. The pressure taps are aligned along both the mid-chord as well as the span at several chordwise locations. Moreover, a total number of 91 dynamic transducers are embedded (i.e. 70 direct sensing and 21 are remote sensing). The former consist of FG-23629-P16 condenser transducers by Knowles placed under a pin hole of 0.4 mm diameter, whereas the remaining latter are fitted with Panasonic WM-61A condenser transducers by in-house designed connections. Figure 2 illustrates the distributions and locations of both the pressure taps and surface dynamic transducers along the chord-wise direction. It should be noted that all transducers were calibrated in magnitude and phase with reference to a G.R.A.S. 40PL mi-

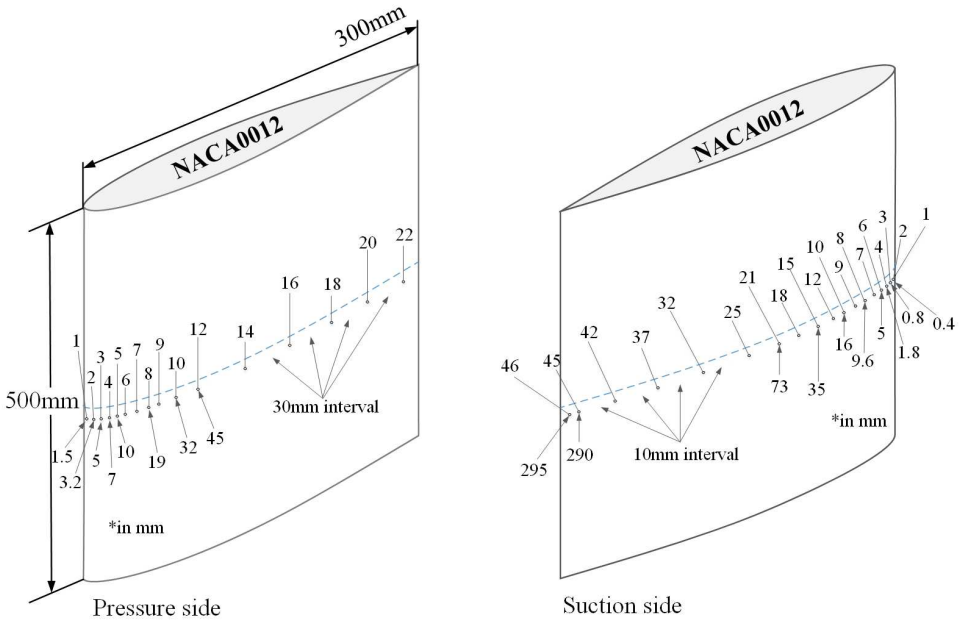

(a) Pressure tap locations along the pressure side and suction side

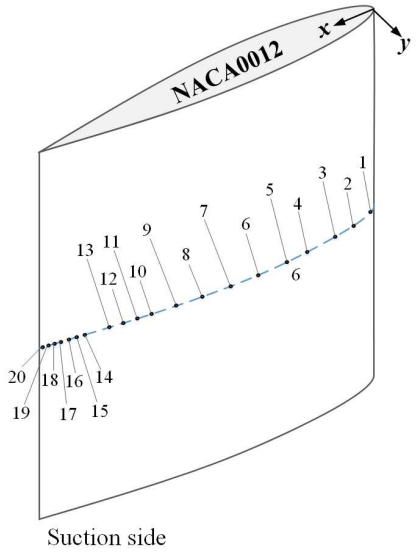

Sensor index	x/C (%)	Sensor index	x/C (%)
1	3.3	11	73.3
2	10.0	12	76.7
3	16.7	13	80.0
4	30.0	14	86.7
5	36.7	15	90
6	48.3	16	93.3
7	53.3	17	95.0
8	60.0	18	96.7
9	66.7	19	98.3
10	70.0	20	99

(b) Direct and remote dynamic transducer locations along the suction side

Figure 2: Chordwise locations of pressure taps and direct/remote transducers along the NACA 0012 aerofoil.

crophone before commencing the actual tests. Readers are advised to refer to the work by Garcia-Sagrado and Hynes,[17] and Liu et al.[18] for more details. On top of the near-field measurements, all far-field noise measurements have been carried out with the overhanging microphone arc, as seen in Figure 1, which is equipped with 23 G.R.A.S. 40PL microphones from polar angle of 35° to 145° at a distance of 9.6 m away from the aerofoil trailing-edge.[16]

For the hot-wire measurements, a Dantec 55P16 single-wire was employed and its data collected through a Dantec StreamlinePro system with a CTA91C10 module. Similarly, the hotwire was calibrated using a Dantec 54H10 calibrator before each run. To achieve a satisfactory convergence on the sampled data, all near- and far-field microphones and the corresponding hotwire measurements were carried out simultaneously at

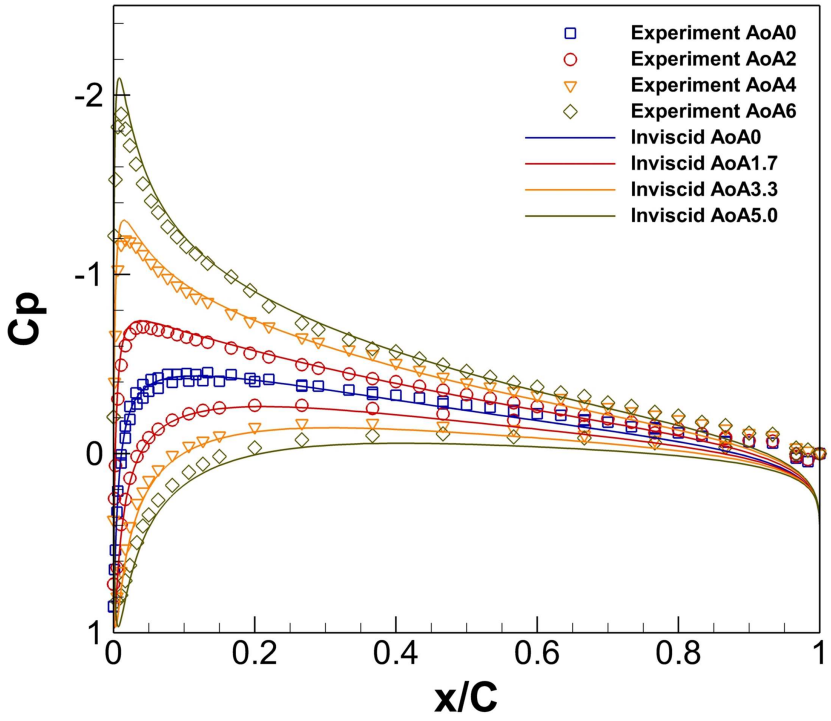

Figure 3: Comparison of measured pressure coefficients at 19.6 m s^{-1} for $\alpha = 0°$, 2°, 4° and 6° with inviscid flow solutions from Xfoil.

a sampling frequency of 2^{15} Hz for 12 s using National Instruments PXIe-4499 modules. Finally, the power spectral density is calculated via Welch's method with a window size of 2^{15} samples and a Hamming window with 50 % overlap. The power spectral density have a frequency bin size of 4 Hz and are normalised with p_0 =20 µPa. The present experiments were conducted with a range of velocities from 9.6 m s^{-1} to 19.6 m s^{-1} at 2 m s^{-1} interval, which correspond to Reynolds numbers, Re_c, from 1.8×10^5 to 4.6×10^5 based on the chord length, similar to that suggested by Arbey and Batalie[12] before critical boundary-layer transition takes place.

III. Results and Discussion

A. Pressure coefficient distributions at $\alpha = 0°$, 2°, 4° and 6°

To first demonstrate the validity of the present experimental setup, the pressure coefficient distributions of the NACA 0012 aerofoil for four AoAs of $\alpha = 0°$, 2°, 4° and 6° at $U = 19.6$ m s^{-1} are shown in Figure 3, together with the inviscid flow solutions calculated from Xfoil. Expectedly, as the AoA increases, the pressure distributions along the pressure and suction surfaces deviate further from each other, with the location of the minimum pressure moving gradually closer toward the leading-edge. Comparing the experimental measurement with the inviscid results obtained from Xfoil, it is clear that some discrepancies exist between the geometric and the simulated AoAs. Nevertheless, considering the relatively small differences between them and the viscous effect at the moderate Reynolds number, it remains reasonable to employ geometric AoA for consistency across all measurements and discussion.

B. Far-field noise measurements at $\alpha = 0°$, 2°, 4° and 6°

The radiated far-field noise spectra of the aerofoil at four different AoAs ($\alpha = 0°$, 2°, 4° and 6°) and flow velocities of $U = 9.6$ m s^{-1} to 23.6 m s^{-1} are shown in Figure 4. Note that definitions of the key frequency peaks, such as f_s, f_n and $f_{n,max}$, have been indicated in Figure 4(a). At $U = 9.6$ m s^{-1}, both a prominent broadband 'hump' with primary frequency of f_s and a set of discrete frequency peaks with the maximal

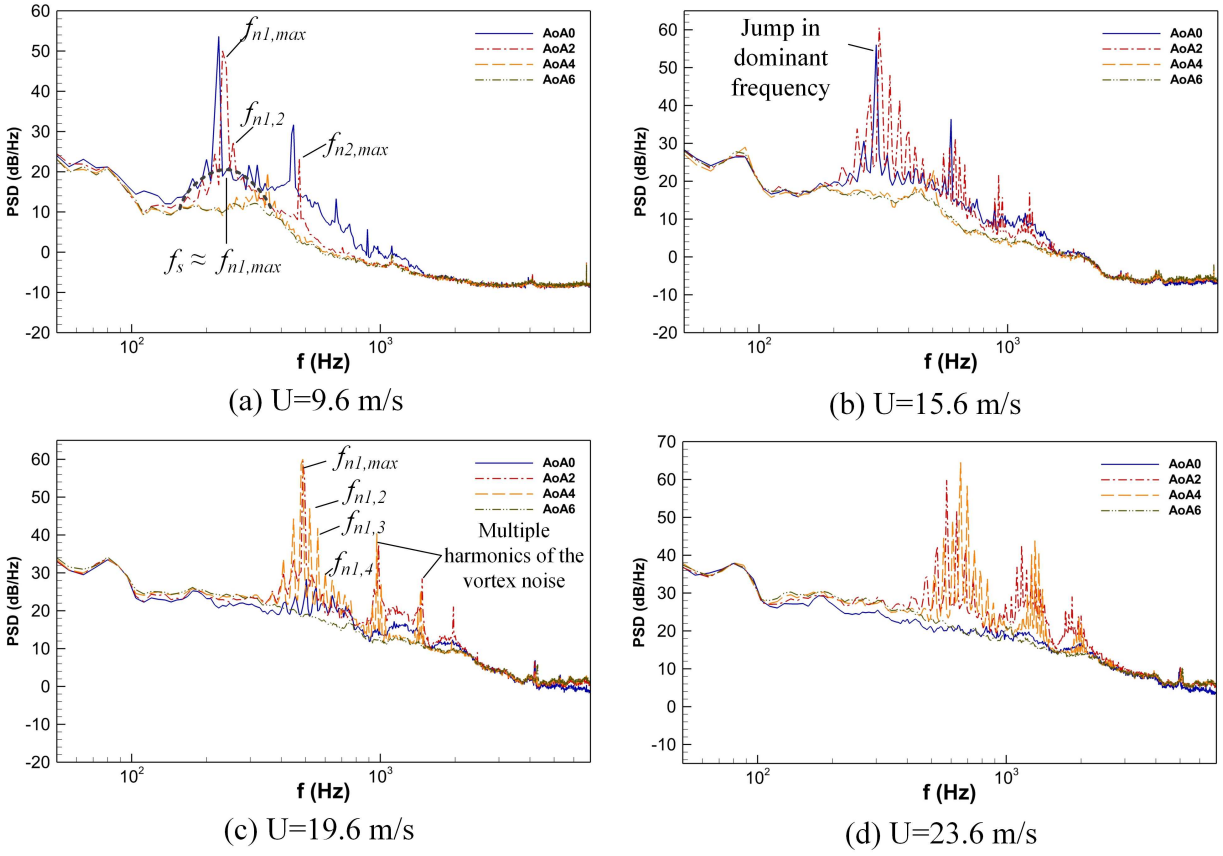

Figure 4: Far-field spectral density of the noise at flow velocities of (a) $U = 9.6\,\mathrm{m\,s^{-1}}$, (b) $U = 15.6\,\mathrm{m\,s^{-1}}$, (c) $U = 19.6\,\mathrm{m\,s^{-1}}$ and (d) $U = 21.6\,\mathrm{m\,s^{-1}}$ for all four AoAs, measured from 90° microphone.

frequency $f_{n,max}$ can be clearly observed with the two peaks coincide very well with each other for the two AoAs (i.e. $\alpha = 0°$ and 2°). This dominant discrete peak is recognized by both Paterson et al.[1] and Arbey and Batalie[12] to be directly associated with the periodic vortex shedding in the wake of the aerofoil. Moreover, the emergence of secondary and tertiary peaks at the multiples of the dominant peak (i.e. the existence of harmonics) across all velocities further confirms that the dominant discrete peak originating from the boundary layer instabilities bears the trademark of vortex noise.[19]

Zooming onto the dominant frequency peak with a set of discrete sub-peaks, the difference between two consecutive discrete peaks (i.e. Δf_n) remains constant for a given AoA and flow velocity - an essential characteristics identified from the noise tones generated by T-S instabilities. For instance, at $U = 13.6\,\mathrm{m\,s^{-1}}$ and $\alpha = 2°$, the four discrete peaks are located at 344 Hz, 376 Hz, 408 Hz and 440 Hz, respectively, with a Δf_n of approximately 32 Hz. This is highly consistent with the results found in the literature.[9,12,14] Table 1 summarizes the discrete peak frequencies f_n and the harmonics of the dominant peak under the present experimental conditions at AoA of $\alpha = 0°$. Interestingly, at a particular flow velocity, the Δf_n(s) are comparable for all AoAs tested under the present study. Furthermore, as the velocity increases, the difference between two consecutive discrete peaks widens. On the other hand, it can be seen from Figure 4 that the magnitude of the dominant discrete frequency $f_{n,max}$ is noticeably greater than the all the sub-peaks. As such, the Tollmien-Schlicting (T-S) instabilities appear to be significantly amplified under the present experimental condition. For clarity, .

Tam[2] argued from the evidence of multiple discrete peaks that a self-excited feedback loop of aerodynamic origin must be present in the wake of the aerofoil near the trailing-edge in order to produce these peaks with relatively constant interval (i.e. an interger phase change condition to be satisfied). Instead of solving the function which depends on the flow velocity and AoA, $g(U, \alpha)$, he demonstrated that the discrete frequencies scaled with $U^{0.8}$. Figure 5 shows an attempt to collapse the present experimental data

onto the proposed 'ladder' structures[1] for the discrete tones. The results scale exceptionally well with $U^{0.8}$ when the integer n is taken at n=4 and 5 for the lower and upper 'rung' at $f = 9.4\,\mathrm{n}U^{0.8}$, respectively, which lends favourable support to the existence of a feedback loop mechanism. Surprisingly however is the fact that the overall trend can be well predicted by $f \sim U^{1.5}$, corroborating with that derived from wake vortex characteristics by Paterson et al.[1]

Table 1: Summary of the discrete tonal frequencies and related harmonics for angle of attack of $\alpha = 0°$ and $U = 9.6\,\mathrm{m\,s^{-1}}$.

Velocity ($\mathrm{m\,s^{-1}}$)	Dominant Peak $f_{n1,max}$ (Hz)	Peak 2 $f_{n1,1}$ (Hz)	Peak 3 $f_{n1,2}$ (Hz)	1^{st} Harmonic $f_{n2,max}$ (Hz)	1^{st} Harmonic $f_{n3,max}$ (Hz)
9.6	224	252	-	448	664
	Δf (Hz)	28	-	224	216
11.6	256	280	308	512	768
	Δf (Hz)	24	28	256	256
13.6	296	328	360	592	-
	Δf (Hz)	32	32	296	-
15.6	376	408	440	744	-
	Δf (Hz)	32	32	368	-
19.6	504	544	584	-	-
	Δf (Hz)	40	40	-	-

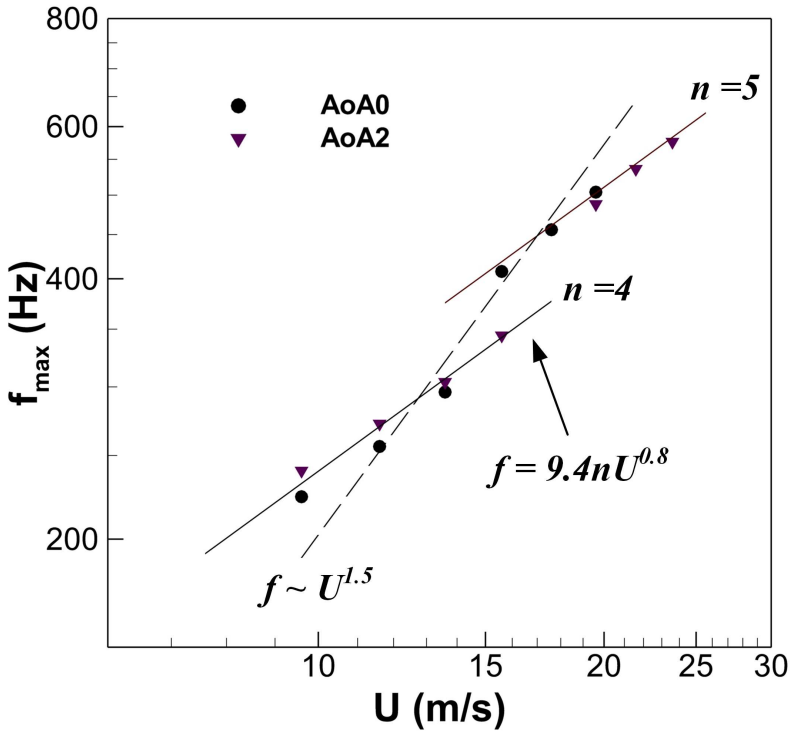

Figure 5: Effect of velocities on the discrete frequency peaks for NACA 0012 with 'ladder' structures scaled with $U^{0.8}$.

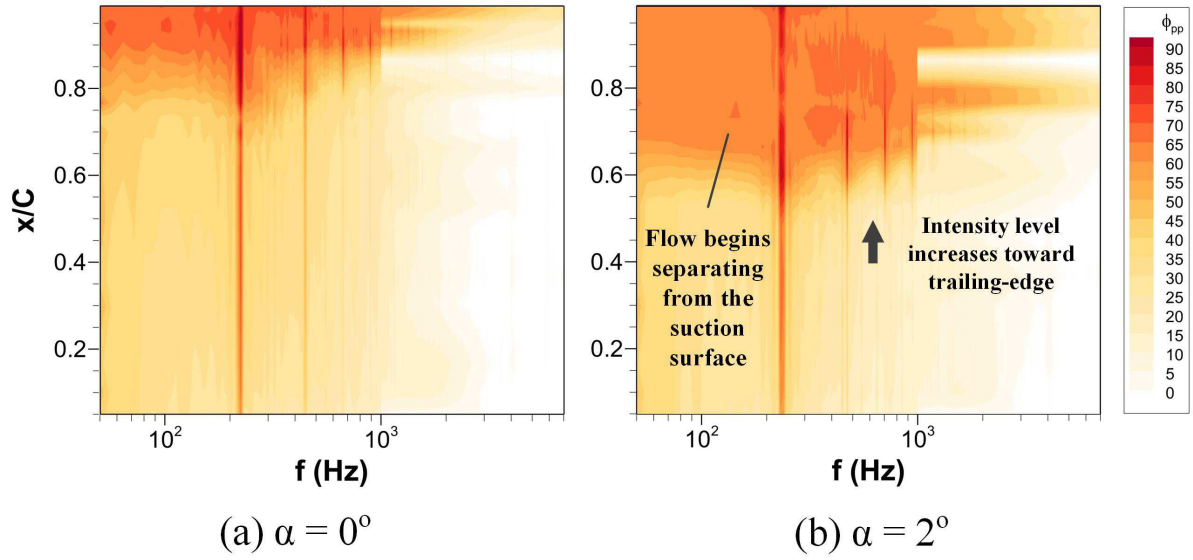

Figure 6: Power spectral density of the near-field pressure fluctuations at AoAs of (a) $\alpha = 0°$ and (b) $\alpha = 2°$ for $U = 9.6\,\mathrm{m\,s^{-1}}$.

C. Near-field pressure spectra

Since the T-S instabilities originate from the laminar boundary-layer over aerofoil and subsequently propagate towards and being diffracted at the trailing-edge,[2,12] the spectra of the surface pressure fuctuations along the aerofoil can provide further information on the evolution of such instabilities. Figure 6 shows the spectral of the pressure fluctuations measured from the surface dynamic transducers along the chord-wise direction. The discrete peaks, as expected, can be clearly observed to span the entire domain, from leading-edge to trailing-edge. Moreover, the intensity level keeps increasing, moving toward the trailing-edge when the flow remains attached to the aerofoil surface whereas becomes relatively constant after the flow begins to separate, as can be identified by comparing Figure 6(a) and (b) at approximately

D. Wake velocity spectra and temporal correlation

Both the far-field and near-field results above demonstrate support to both proposed mechanisms associated with the tones generated by T-S instabilities. To further investigate and understand the phenomenon, the wake velocity spectra for AoAs 0° and 2° at flow velocities of $U = 9.6\,\mathrm{m\,s^{-1}}$ and $U = 15.6\,\mathrm{m\,s^{-1}}$ are shown in Figure 7, respectively. It can be observed clearly that both the dominant discrete tone (224 Hz) and its first harmonic (454 Hz) captured by the far-field microphones are equally notable in the wake velocity spectra. Note that the density spectra of the wake velocities are obtained in a similar manner to those from the microphone and surface transducer measurements. for all downstream locations. Although the tonal intensity abates gradually from $x/C = 0.7\,\%$ to $x/C = 53\,\%$, suggesting that the wake structures are convecting away from the noise source, the discrete tone and its harmonics persist through a relatively long distance downstream. It agrees with the fact that wake vortex roll-ups convects sufficiently far from the aerofoil trailing-edge, simultaneously carrying the disturbances from the hydrodynamic instabilities. Increasing both the AoA to 2° and flow velocity to $U = 15.6\,\mathrm{m\,s^{-1}}$ sees a similar trend, which the the dominant tone and its first harmonic can be observed at all downstream locations in the wake velocity spectra. Consequently, despite the fact that the wake vortex phenomenon can hardly account for the appearance of fine structures in the noise measurements (recall from Figure 4 on the discrete sub-peaks), the wake velocity spectra connects strongly the dominant tone to that of the vortex noise from the aerofoil trailing-edge.

In addition to the prominent tonal peaks, a careful examination indicates the presence of minor, and yet noticeable peaks scattered around that of the dominant ones, which could indicate that fine structures also being captured in the wake velocity spectra up to approximately $x/C = 16\,\%$ downstream of the trailing-edge. To have a better insight into these sub-peaks and the possible physical mechanisms associated with

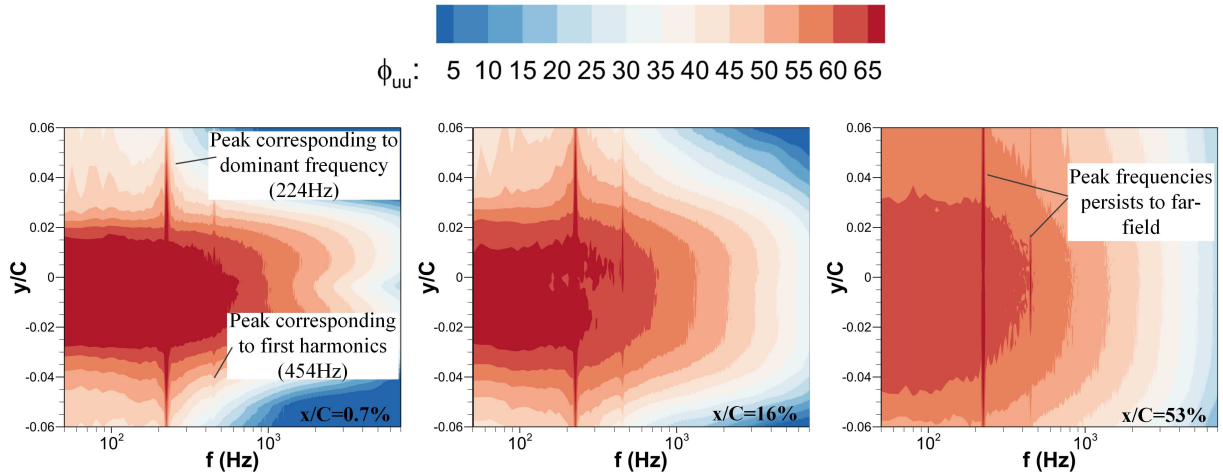

(a) Power spectral density of the wake velocity measurement at U=9.6ms and AoA0

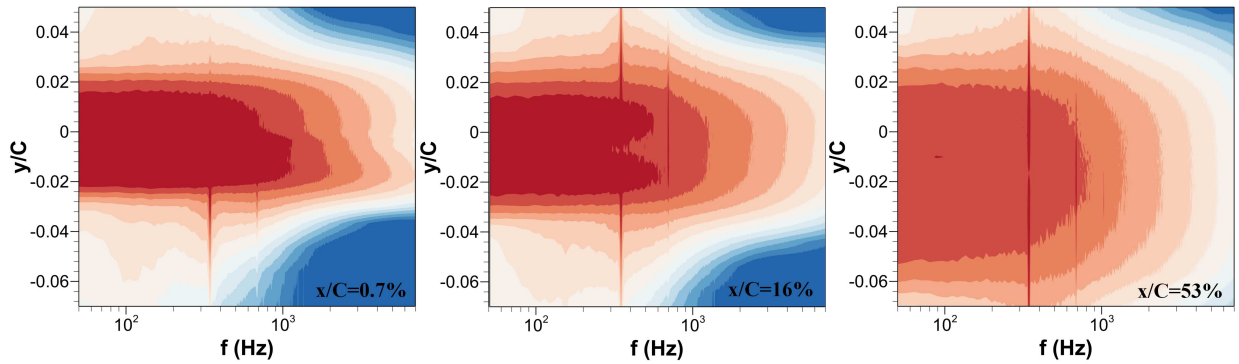

(b) Power spectral density of the wake velocity measurement at U=15.6ms and AoA2

Figure 7: Wake velocity spectral contours at (a) AoA of $\alpha = 0°$, $U = 9.6\,\mathrm{m\,s^{-1}}$ and (b) AoA of $\alpha = 2°$, $U = 15.6\,\mathrm{m\,s^{-1}}$.

them, temporal correlation between the selected surface transducers and the wake velocity measurements are depicted in Figure 8. The temporal correlation coefficient,$R_{p'u'}$, is defined as:

$$R_{p_i' u_j'}(\tau) = \frac{\overline{p_i'(x_i, t+\tau) u_j'(x_j, t)}}{p_{i'_{rms}}(x_i) u_{j'_{rms}}(x_j)}, \tag{1}$$

where p_i' and u_j' are the simultaneous temporal signals collected by the surface transducers and hotwire probe at locations of (x_i, y_i) and (x_j, y_j), respectively, $p_{i'_{rms}}$ and $u_{j'_{rms}}$ are the root-mean-square of the pressure and velocity fluctuations and τ denotes the time delay between the two signals. The calculations follow closely to those employed by Showkat Ali et al.[20] Two surface transducers, located at 30 % and 90 % of the chord, respectively, are shown with each correlated to the wake velocity measurements at $x/C = 0.7\,\%$, $x/C = 16\,\%$ and $x/C = 53\,\%$ downstream. Several noteworthy features can be drawn from the temporal correlation results. Firstly, periodic convection of large-scale structures can be observed, commencing from the aerofoil trailing-edge. This is in excellent agreement with the direct numerical simulation study by Desquesnes et al.,[14] whereby their simulation results showed distinct vortex roll-ups from the instabilities close to the trailing-edge. Secondly, significant correlations even exist between the wake and surface transducer at 30 % chord upstream, reassuring that the dominant tones are indeed manifestation of hydrodynamic instabilities (i.e. the T-S instabilities). It is also worthwhile to mention that the level of correlation increases moving from transducer at $x/C = 30\%$ to that at 90% of the chord, which indicates the location of the noise source being close to the trailing-edge. Thirdly, time lag ($\Delta\tau$) between consecutive structures, as indicated in

Figure 8(a), is found to be 0.0044 s, corresponding to a frequency of 227 Hz. As such, it can be concluded that the periodic structures obtained from the temporal correlation between surface transducer and wake measurements are directly related to the dominant tone under the present investigation. Most importantly, there is a clear reverse in the phase of the convecting structures at approximately $x/C = 16\,\%$, providing further and meaningful confirmation to the feedback loop proposed by Tam,[2] who postulated that the noise source is likely to be located at the aerofoil wake, close to that of the trailing-edge and of aerodynamic origin.

E. Harmonics of the dominant tone

Indeed, the characteristics of the aerofoil noise produced from T-S instabilities can be a combination of the vortex noise and presence of a near-wake feedback loop. There have been several other notable attempts to reconcile the mechanisms and advance further the understanding on the tonal noise. For instance, Arbey and Batalie[12] modified the feedback mechanism to include the characteristic length to account for the boundary layer transition along aerofoil surface flow separation and Probsting et al.[15] suggested the necessity to consider dual feedback, each responsible for a side of the aerofoil surface. Nevertheless, there have been quite limited attention on the presence of the harmonics of the dominant tone and the role that they play on the modulation of the instabilities and/or fine structures.

Last but not least, Figure 9 shows the enclosed region where harmonics of the primary tone are present under the present experimental conditions. A quick survey from Figure 9 reveals that discrete sub-peaks can also be observed at these harmonics, with a Δf_n comparable to that of its dominant counterparts. Therefore, it may warrant further studies into this aspect of the noise spectra.

IV. Concluding remark

A series of experimental measurements have been carried out in the aeroacoustic wind tunnel facility to investigate the development of Tollmiem-Schlicting instabilities and its associated aerofoil noise for a NACA 0012 profile at moderate Reynolds number. From the selected four AoAs ($\alpha = 0°$, $2°$, $4°$ and $6°$) and a range of free-stream velocities from $U = 9.6\,\mathrm{m\,s^{-1}}$ to $23.6\,\mathrm{m\,s^{-1}}$. The far-field noise spectra exhibit characteristics of the aerofoil noise produced from T-S instabilities with a dominant discrete tone accompanied with multiples of sub-peaks as well as its harmonics.

An attempt made to examine the effect of velocity on the discrete tone points the presence of a 'ladder' structure, which scales well with the feedback loop mechanism ($\sim U^{0.8}$) proposed by Tam[2] with the overal trend scaling satisfactorily with that derived from wake vortex theory by Paterson et al.[1] ($\sim U^{1.5}$). Such interesting results prompt further investigations of the wake velocity spetra as well as the temporal correlation between the surface transducers and wake velocity measurements. The wake spectral reveal persistent existence of tonal peaks in the wake at both the dominant and its first harmonic frequencies beyond $x/C = 53\,\%$ downstream of the aerofoil trailing-edge, corroborating with the arguments put forward by Paterson et al.[1] On the other hand, the temporal correlation detects a phase reversal close to the aerofoil trailing-edge, indicating the possible existence of the noise source in the wake, close to the trailing-edge, as qualitatively analyzed by Tam.[2] Consequently, the two mechanisms both have merits in elucidating the part of the noise spectra from T-S instabilities. Hence, a more extensive investigation could help shed further lights into the their dynamic interactions.

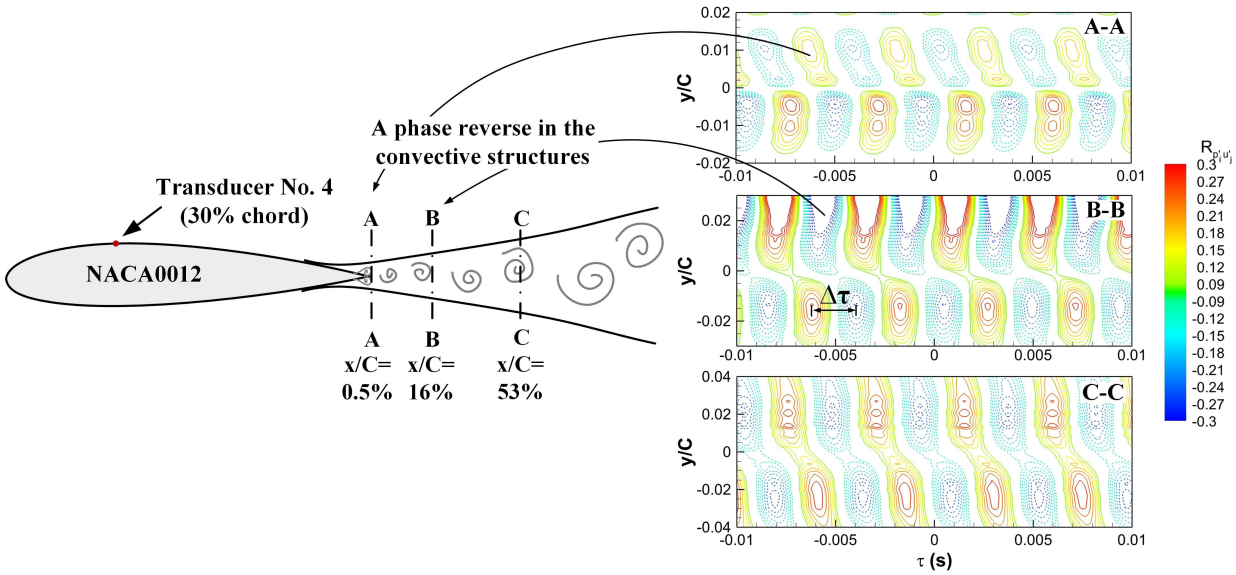

(a) Cross-correlation map between surface dynamic transducer (30% chord) and hot-wire measurements along downstream stations (A-A, B-B and C-C)

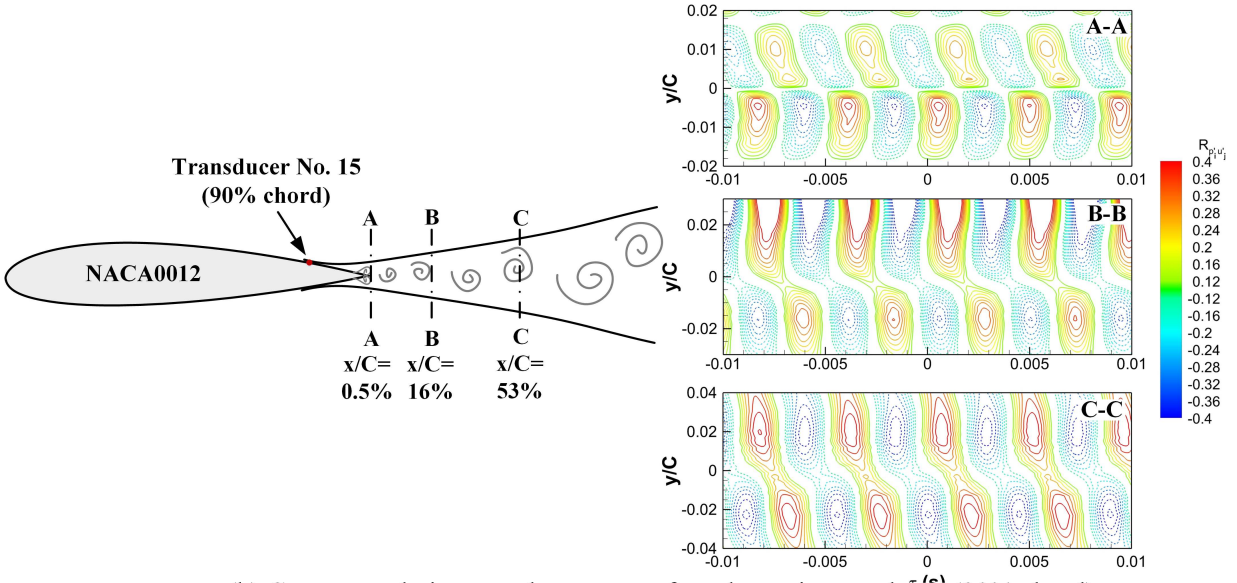

(b) Cross-correlation map between surface dynamic transducer (90% chord) and hot-wire measurements along downstream stations (A-A, B-B and C-C)

Figure 8: Temporal correlations between surface dynamic transducers (a) at $x/C = 30\%$ chord and (b) at $x/C = 30\%$ chord with the wake velocity measaurements for AoA of $\alpha = 2°$ and $U = 15.6\,\mathrm{m\,s^{-1}}$. Note that contours are depicted at three downstream locations of x/C=0.7%, 16% and 53% from the trailing-edge.

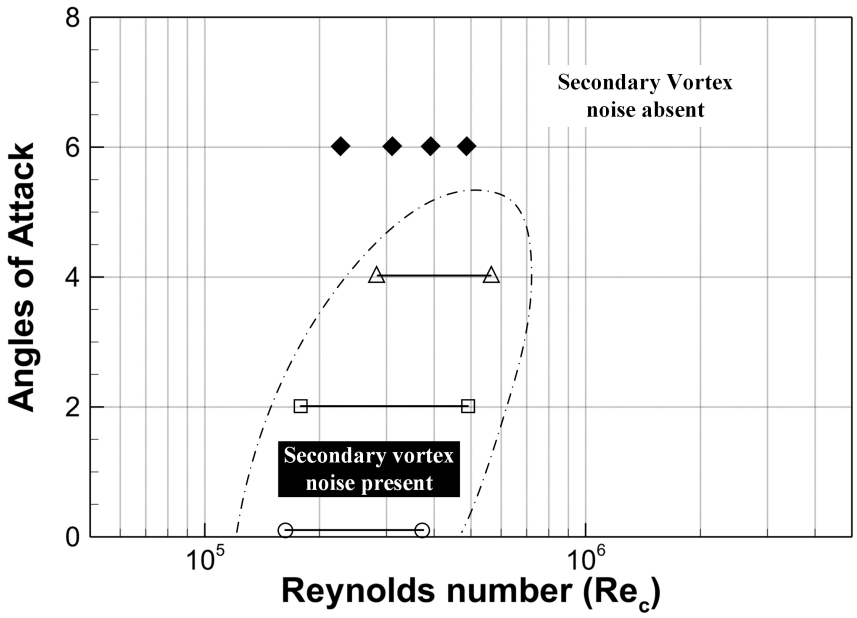

Figure 9: Identified region with presence and absence of the harmonics of the dominant tone under the present experimental conditions.

Acknowledgement

The authors would like to acknowledge EPSRC for the suport of the present study.

References

[1]Paterson, R. W., Vogt, P. G., Fink, M. R., and Munch, C. L., "Vortex noise of isolated airfoils," *Journal of Aircraft*, Vol. 10, No. 5, 1973, pp. 296–302.

[2]Tam, C. K. W., "Discrete tones of isolated airfoils," *The Journal of the Acoustical Society of America*, Vol. 55, No. 6, 1974, pp. 1173–1177.

[3]Clark, L. T., "The radiation of sound from an airfoil immersed in a laminar flow," *Journal of Engineering for Power*, Vol. 93, No. 4, 1971, pp. 366–376.

[4]Hersh, A. S. and Hayden, R. E., "Aerodynamic sound radiation from lifting surfaces with and without leading-edge serrations," *Technical Report NASA CR-114370*, 1971.

[5]Fink, M. R., "Prediction of airfoil tone frequencies," *Journal of Aircraft*, Vol. 12, No. 2, 1975, pp. 118–120.

[6]Arcondoulis, E. J. G., Doolan, C. J., Zander, A. C., and Brooks, L. A., "A review of trailing edge noise generated by airfoils at low to moderate Reynolds number," *Acoustics Australia Bulletin*, Vol. 38, No. 3, 2010.

[7]Nash, E. C. and Lowson, M. W., "Noise due to boundary layer instabilities," *1st CEAS/AIAA Joint Aeroacoustics Conference*, Munich, Germany, 1995, pp. 875–884.

[8]Nash, E. C., Lowson, M. V., and McAlpine, A., "Boundary-layer instability noise on aerofoils," *Journal of Fluid Mechanics*, Vol. 382, 1999, pp. 27–61.

[9]Plogmann, B., Herrig, A., and Würz, W., "Experimental investigations of a trailing edge noise feedback mechanism on a NACA 0012 airfoil," *Experiments in fluids*, Vol. 54, No. 5, 2013, pp. 1480.

[10]Herr, M. and Dobrzynski, W., "Experimental Investigations in Low-Noise Trailing Edge Design," *AIAA journal*, Vol. 43, No. 6, 2005, pp. 1167–1175.

[11]Chong, T. P., Vathylakis, A., Joseph, P. F., and Gruber, M., "Self-noise produced by an airfoil with nonflat plate trailing-edge serrations," *AIAA journal*, Vol. 51, No. 11, 2013, pp. 2665–2677.

[12]Arbey, H. and Bataille, J., "Noise generated by airfoil profiles placed in a uniform laminar flow," *Journal of Fluid Mechanics*, Vol. 134, 1983, pp. 33–47.

[13]Lowson, M., Fiddes, S., and Nash, E., "Laminar boundary layer aero-acoustic instabilities," *32nd Aerospace Sciences Meeting and Exhibit*, Reno, Nevada, United States, 1994, p. 358.

[14]Desquesnes, G., Terracol, M., and Sagaut, P., "Numerical investigation of the tone noise mechanism over laminar airfoils," *Journal of Fluid Mechanics*, Vol. 591, 2007, pp. 155–182.

[15]Pröbsting, S., Scarano, F., and Morris, S., "Regimes of tonal noise on an airfoil at moderate Reynolds number," *Journal of Fluid Mechanics*, Vol. 780, 2015, pp. 407–438.

[16]Mayer, Y., Kamliya Jawahar, H., Szoke, M., and Azarpeyvand, M., "Design of an Aeroacoustic Wind Tunnel Facility at the University of Bristol," *2018 AIAA/CEAS Aeroacoustics Conference*, Atlanta, Georgia, United States, 2018.

[17]Garcia-Sagrado, A. and Hynes, T., "Wall pressure sources near an airfoil trailing edge under turbulent boundary layers," *Journal of Fluids and Structures*, Vol. 30, 2012, pp. 3–34.

[18]Liu, X., Showkat Ali, S. A., and Azarpeyvand, M., "On the application of trailing-edge serrations for noise control from tandem airfoil configurations," *23rd AIAA/CEAS Aeroacoustics Conference*, AIAA 2017-3716, Stockholm, Sweden, 2017.

[19]King, W. F. and Pfizenmaier, E., "An experimental study of sound generated by flows around cylinders of different cross-section," *Journal of Sound and Vibrations*, Vol. 328, 2009, pp. 318–337.

[20]Showkat Ali, S. A., Azarpeyvand, M., and Ilário da Silva, C. R., "Trailing-edge flow and noise control using porous treatment," *Journal of Fluid Mechanics*, Vol. 850, 2018, pp. 83–119.